Density Functional Study of the Mechanism of C≡C, O−H, and N−H Bond Activation at the Pd═X (X = Sn, Si, C) Bonds of the $(PH_3)_2Pd═XH_2$ Complexes

Toshiaki Matsubara*

Institute for Fundamental Chemistry, 34-4 Takano-Nishihiraki-cho, Sakyo-ku, Kyoto 606-8103, Japan

Received November 22, 2000

The mechanism of the activation of the C≡C π bond of ethyne, the O−H bond of water, and the N−H bond of ammonia at the Pd═X (X = Sn, Si, C) bonds of the model $(PH_3)_2Pd═XH_2$ complexes **1** to produce the products $(PH_3)_2Pd(CH═CH)XH_2$ (*Pd−X*) **4**, $(PH_3)_2Pd(H)X(OH)H_2$ **7**, $(PH_3)_2Pd(H)X(NH_2)H_2$ **9**, respectively, has been theoretically investigated using a density functional method (B3LYP). The reaction mechanism significantly depends on both substrate and atom X of the complex **1**. In the activation of the C≡C π bond of ethyne at the Pd═Sn bond, a weak η^2-interaction of the C≡C π bond not with Pd but with Sn initiates the reaction. The rotation of the $(PH_3)_2Pd$ group around the Pd−Sn axis makes the reaction facile so that a small energy barrier of only 6.2 kcal/mol is required. Although the reaction at the Pd═Si bond also takes the same mechanism, the reaction is downhill without energy barrier. On the other hand, when X is C, the reaction proceeds by a completely different mechanism without the coordination of the C≡C π bond to the C atom. In the activation of the O−H bond of water at the Pd═Sn bond, after the coordination of the H_2O oxygen to the Sn atom, the O−H bond is heterolytically broken and the hydrogen is transferred to the Pd atom as a proton with an energy barrier of 16.9 kcal/mol. The same heterolytic cleavage takes place at the Pd═Si bond, requiring a smaller energy barrier, while at the Pd═C bond the homolytic cleavage takes place without the coordination of the H_2O oxygen to the C atom. In the case of NH_3, independent of the atom X, heterolytic cleavage of the N−H bond occurs after coordination of the NH_3 nitrogen to the X atom and the transfer of a hydrogen as a proton to the Pd atom. The large energy barrier of 33.2 kcal/mol required in the reaction system with X = Sn for which no activation activity has been experimentally observed was reduced to half in the reaction system with X = C, suggesting an activation activity. The factors that determine the activation mechanism are discussed.

1. Introduction

The breaking and formation of specific bonds of organic compounds under mild conditions have been a challenging subject for organic chemists for a long time. Especially, the activation of H−H, C−H, Si−H, C−C, and Si−Si bonds and so on, which is an important elementary step in catalytic organic syntheses, has been extensively studied. Remarkable development in this area has been attained with transition metal complexes over the last two decades.[1] Most of such reactions experimentally reported proceed in a homogeneous system with mononuclear complexes because the reaction can be controlled with a high efficiency, suppressing byproducts. The numerous theoretical investigations for the energetics as well as the structures of the intermediates and transition states using ab initio molecular orbital (MO) methods have clarified their activation mechanism.[2]

For example, the breaking of the H−H bond by the oxidative addition to the phosphine-coordinated $(PH_3)_2M$ (M = Pd, Pt) complexes with the linear P−M−P axes passes through an early square-planar transition state where the slightly activated H_2 molecule is bound to the metal parallel to the P−M−P plane made by the bent P−M−P axis by the side-on configuration to produce the *cis*-$(PH_3)_2M(H)_2$ complexes.[3,4] It is generally well known that the σ (or π) bond breaking on a metal site takes place by two kinds of molecular orbital interactions between the σ (or π) bond and the metal: (i) electron

(1) For example, see: (a) Muetterties, E. L.; Rhodin, T. N.; Band, E.; Brucker, C. F.; Pretzer, W. R. *Chem. Rev.* **1979**, *79*, 91. (b) Shilov, A. E. *The Activation of Saturated Hydrocarbons by Transition Metal Complexes*; D. Reidel: Dordrecht, 1984. (c) Crabtree, R. H. *Chem. Rev.* **1985**, *85*, 245. (d) Cotton, F. A.; Wilkinson, G. In *Advanced Inorganic Chemistry*, 5th ed.; John Wiley & Sons: New York, 1988. (e) Crabtree, R. H. In *The Organometallic Chemistry of the Transition Metals*, 2nd ed.; John Wiley & Sons: New York, 1994.

(2) For example, see: (a) Koga, N.; Morokuma, K. *Chem. Rev.* **1991**, *91*, 823. (b) Hay, P. J. In *Transition Metal Hydrides*; Dedieu, A., Ed.; VCH: New York, 1992. (c) Siegbahn, P. E. M.; Blomberg, M. R. A. In *Theoretical Aspects of Homogeneous Catalysis*; van Leeuwen, P. W. N. M., Morokuma, K., van Lenthe, J. H., Eds.; Kluwer Academic Publishers: Dordrecht, 1995. (d) Musaev, D. G.; Morokuma, K. In *Advances in Chemical Physics*; Prigogine, I., Rice, S. A., Eds.; John Wiley & Sons: New York, 1996; Vol. XCV.

(3) (a) Kitaura, K.; Obara, S.; Morokuma, K. *J. Am. Chem. Soc.* **1981**, *103*, 2891. (b) Obara, S.; Kitaura, K.; Morokuma, K. *J. Am. Chem. Soc.* **1984**, *106*, 7482.

(4) (a) Low, J. J.; Goddard, W. A., III. *J. Am. Chem. Soc.* **1984**, *106*, 6928. (b) Low, J. J.; Goddard, W. A., III. *J. Am. Chem. Soc.* **1984**, *106*, 8321.

10.1021/om001000a CCC: $20.00
Publication on Web 03/08/2001

donation from the σ (or π) orbital of the σ (or π) bond to the dσ(+sp) orbital of the metal, and (ii) back-donation from the dπ orbital of the metal to the σ^* (or π^*) orbital of the σ (or π) bond. Thus, the H−H bond is initially activated by electron donation from the H−H σ orbital to the hybridized dσ+sp orbital of the metal and is broken by π-back-donation from the dπ orbital of the metal to the H−H σ^* orbital as presented below. The

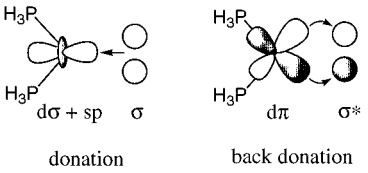

dπ orbital of the metal in the P−M−P plane is enhanced by the bend of the P−Pd−P axis to interact with the H−H σ^* orbital, so that the H−H bond is parallel to the P−M−P plane throughout the reaction.

In the C−H and Si−H bond breaking by the T-shaped three-coordinated $Cl(PH_3)_2Rh$ species, where the two phosphine ligands are trans to each other, the available dπ orbital for the electron back-donation to the σ^* orbitals of the C−H and Si−H bonds is perpendicular to the $Cl(PH_3)_2Rh$ plane. Therefore, the reaction passes through a trigonal-bipyramidal transition state with the C−H or Si−H bond bound to the empty site perpendicular to the $Cl(PH_3)_2Rh$ plane.[5] On the other hand, the four-coordinated square-planar complexes, such as *trans*-$IrCl(CO)(PH_3)_2$ or *cis*-$IrCl(CO)(PH_3)_2$, show a butterfly structure in the transition state where the two trans ligands of four ligands are bent back to interact with the incoming H_2 molecule by the side-on approach.[6] However, the piano-stool type complex, for example CpRh(L), shows no essential structural change in the activation of H−H, C−H, O−H, and N−H bonds,[7] because its initial structure already has the same frontier molecular orbitals as those of the butterfly structure of the four-coordinated complex; that is, these species are isolobal to each other.[8]

In the previous paper, we also reported that the activation of the aromatic C−H bond by the phosphine-coordinated Ru complex proceeds by the novel mechanism consisting of two steps via a cyclometalated intermediate;[9] in the first step, the Ru−C bond is formed without the activation of the C−H bond, where the Ru atom is oxidized from Ru(0) to Ru(II), and in the second step, the H atom is transferred to the Ru atom, where the oxidation number of Ru is unchanged.

The transition metal−tin complexes have also attracted much attention from many chemists because of their unique properties and activities in the syntheses of organic compounds.[10,11] Recently, the catalytic stannole formation by a [2+2+1] cycloaddition reaction of two ethynes and one stannylene, SnR'_2 (R′ = CH(SiMe$_3$)$_2$ and R'_2 = {C(SiMe$_3$)$_2$CH$_2$}$_2$), with the phosphine-coordinated palladium complexes $(PR_3)_2Pd$ and $(R_2PC_2H_4PR_2)Pd$ (R = Me, i-Pr, t-Bu) at a low temperature was experimentally reported by Pörschke and coworkers.[12] In the previous paper, we theoretically examined by the ab initio MO method using the model complexes $(PH_3)_2M$ (M = Ni, Pd, Pt) the possible reaction path of the catalytic cycle and observed that in the first process of the catalytic cycle the 1,2-metallastannete intermediate, $(PH_3)_2M(CH{=}CH)SnH_2$ (*M*−*Sn*), is formed by the activation of the ethyne C≡C π bond at the Pd═Sn bond after the formation of the stannylene complex $(PH_3)_2M{=}SnH_2$.[13] Pörschke et al. also experimentally reported the activation of the O−H bond of water and methanol at the Pd═Sn bond of the $(R_2PC_2H_4PR_2)Pd{=}SnR'_2$ (R = i-Pr, t-Bu; R′ = CH(SiMe$_3$)$_2$) complexes.[14] The reaction proceeds within a few minutes even at −40 °C to form the $(R_2PC_2H_4PR_2)$-Pd(H)Sn(OR″)R′$_2$ (R″ = H, Me) complexes. However, no reaction of the $(R_2PC_2H_4PR_2)Pd{=}SnR'_2$ complexes takes place with NH_3 under the same conditions, although the NH_3 and the other adducts, $(C_2H_4)Ni{-}SnR'_2$(donor) [donor = THF, NH_3, py, $(Me_2N)_3PO$], have been independently observed.[15] Thus, the activation of various bonds at the double bond between the metal and ligand is unique, and the role of the ligand in the activation reaction is quite interesting.

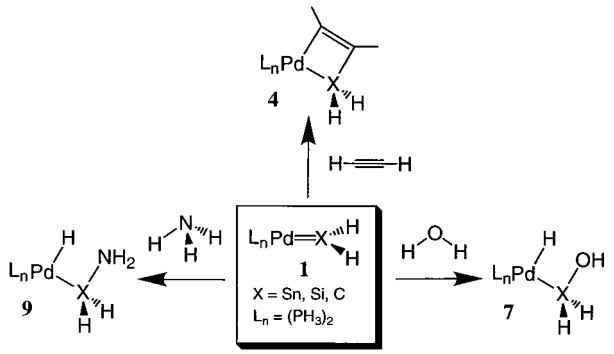

Figure 1. Activation of the C≡C π bond of ethyne, the O−H bond of water, and the N−H bond of ammonia at the Pd═X (X = Sn, Si, C) bonds of the $L_nPd{=}XH_2$ complexes **1**.

In the present study, therefore, the activation of the C≡C π bond of ethyne, the O−H bond of water, and the N−H bond of ammonia at the Pd═X (X = Sn, Si, C) bonds of the stannylene, silylene, and carbene complexes displayed in Figure 1 has been theoretically investigated by the density functional method (B3LYP) using the model complexes $(PH_3)_2Pd{=}XH_2$. Following the explanation of the calculation method in section 2, we will first discuss the stannylene, silylene, and carbene complexes in section 3.1 and then the activation of the

(5) (a) Koga, N.; Morokuma, K. *J. Phys. Chem.* **1990**, *94*, 5454. (b) Koga, N.; Morokuma, K. *J. Am. Chem. Soc.* **1993**, *115*, 6883.

(6) (a) Sargent, A. L.; Hall, M. B. *Inorg. Chem.* **1992**, *31*, 317. (b) Sargent, A. L.; Hall, M. B.; Guest, M. F. *J. Am. Chem. Soc.* **1992**, *114*, 517.

(7) Musaev, D. G.; Morokuma, K. *J. Am. Chem. Soc.* **1995**, *117*, 799.

(8) Elian, M.; Hoffmann, R. *Inorg. Chem.* **1975**, *14*, 1064.

(9) (a) Matsubara, T.; Koga, N.; Musaev, D. G.; Morokuma, K. *J. Am. Chem. Soc.* **1998**, *120*, 12692. (b) Matsubara, T.; Koga, N.; Musaev, D. G.; Morokuma, K. *Organometallics* **2000**, *19*, 2318.

(10) Abel, E. W. *Comprehensive Inorganic Chemistry*; Pergamon Press: Oxford, 1973; Vol. 2, p 43.

(11) Holt, M. S.; Wilson, W. L.; Nelson, J. H. *Chem. Rev.* **1989**, *89*, 11.

(12) (a) Krause, J.; Pluta, C.; Pörschke, K.-R.; Goddard, R. *J. Chem. Soc., Chem. Commun.* **1993**, 1254. (b) Krause, J.; Haack, K.-J.; Pörschke, K.-R.; Gabor, B.; Goddard, R.; Pluta, C.; Seevogel, K. *J. Am. Chem. Soc.* **1996**, *118*, 804.

(13) Sahnoun, R.; Matsubara, T.; Yamabe, T. *Organometallics* **2000**, *19*, 5661.

(14) Schager, F.; Seevogel, K.; Pörschke, K.-R.; Kessler, M.; Krüger, C. *J. Am. Chem. Soc.* **1996**, *118*, 13075.

(15) Pluta, C.; Pörschke, K.-R.; Mynott, R.; Betz, P.; Krüger, C. *Chem. Ber.* **1991**, *124*, 1321.

C≡C π bond in section 3.2, O−H bond activation in section 3.3, and N−H bond activation in section 3.4. The structural features of the equilibrium structures and the transition states and the energetics were quite similar for the activation of the O−H bond of water and methanol at the Pd═Sn bond, as mentioned in section 3.3. The model complex with a chelate ligand, $(H_2C_2H_4PH_2)Pd{=}SnH_2$, was also used for the C≡C and O−H bond activation. Conclusions are given in the last section.

2. Computational Details

All calculations were performed using the Gaussian98 program.[16] The calculations of energetics as well as geometry optimizations were carried out at the B3LYP level of theory, which consists of a hybrid Becke + Hartree−Fock exchange and Lee−Yang−Parr correlation functional with nonlocal corrections,[17] using the basis set I. In the basis set I, the 6-31G** level was used for H, C, N, O, and Si atoms of ethyne, water, methanol, ammonia, stannylene, silylene, and carbene molecules. For the spectator ligands, PH_3 and $H_2PC_2H_4PH_2$, the 6-31G level for C and H atoms and the 6-31G* level for P atoms were used. For Pd and Sn, the triple-ζ (5s,6p,4d,1f)/[3s,3p,3d,1f] augmented by an additional single set of f orbitals with the exponent of 1.472[18] and the effective core potential (ECP) determined by Hay and Wadt[19] to replace the core electrons except the 18 electrons in the valence shell, and the (3s,3p)/[2s,2p] basis functions with a 5d polarization function with the exponent of 0.183[20] and the Hay−Wadt ECP[21] to replace the core electrons except the 4 valence electrons were used, respectively.

All equilibrium structures and transitions states were optimized without any symmetry restrictions and identified by the number of imaginary frequencies calculated from the analytical Hessian matrix. No symmetry was found unless otherwise indicated. The reaction coordinates were followed from the transition state to the reactant and the product by the intrinsic reaction coordinate (IRC) technique.[22] In all cases, the calculated energies relative to the free molecules and $(PH_3)_2Pd{=}SnH_2$ fragment are presented.

3. Results and Discussion

3.1. Stannylene, Silylene, and Carbene Complexes. To know the character of the Pd═X (X = Sn, Si, C) bonds of the starting complexes $(PH_3)_2Pd{=}XH_2$ **1**, which would significantly affect the activation reactions, the interaction of the stannylene, silylene, and carbene fragments with the $(PH_3)_2Pd$ counterpart will be discussed first in this section. The optimized structures of the stannylene, silylene, and carbene complexes **1** are presented in Figure 2.

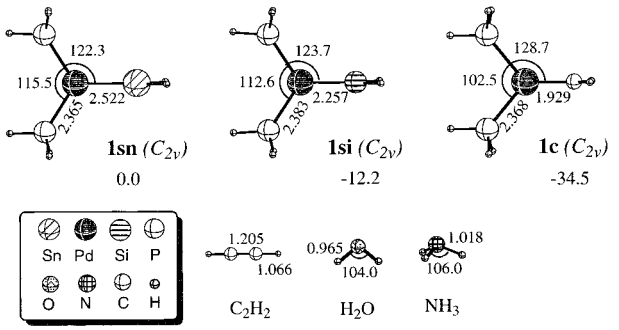

Figure 2. B3LYP/I-optimized structures (in Å and deg) of the stannylene (**1sn**), silylene (**1si**), and carbene (**1c**) complexes, and the free ethyne, water, and ammonia molecules, and their relative energies (in kcal/mol) at the B3LYP/I level.

All the complexes **1sn**, **1si**, and **1c** have a triangular-planar structure with C_{2v} symmetry. It is generally considered that the interaction between the Pd atom and the XH_2 fragment in **1** is well expressed by the electron donation and back-donation as presented below, i.e., the σ-donation of the lone pair electron of the X atom to the hybridized ds+sp orbital of the Pd atom and the π-back-donation from the occupied dπ orbital of the Pd atom to the unoccupied pπ orbital of the X atom. The

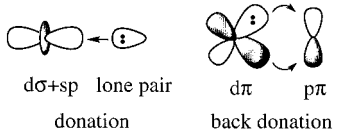

unoccupied pπ orbital of Sn interacts with the occupied dπ orbital of Pd enhanced by the bend of the P−M−P axis.[23] As a result, the H−Sn−H plane is perpendicular to the P−M−P plane. Therefore, the order of the ∠P−M−P angle, Sn > Si > C, indicates that the dπ orbital of Pd which interacts with the pπ orbital of X is enhanced with the opposite order and the π-back-donation becomes stronger in the order C > Si > Sn. The strength of the π-back-donation is evidently reflected in the stability of the complex **1**, of which sequence, C > Si > Sn, coincides with the sequence of the strength of the π-back-donation. The gross orbital population for the pπ orbital of the X atom in **1** consistently increased in the order C(0.995 e) > Si(0.778 e) > Sn(0.290 e). On the other hand, it is considered that the strength of the σ-donation has the opposite order, Sn > Si > C, as shown by the sum of gross orbital populations for the s and p orbitals of X which contribute to the σ-donation in the order C(2.818 e) > Si(2.678 e) ≥ Sn(2.671 e), which is roughly in accordance with the fact that the electronegativity increases in the order C(2.55) > Sn(1.96) ≥ Si(1.90).[24] The carbene complexes can be generally classified in either of two types of complexes, i.e., Fischer[25] and Schrock,[26] according to the

(16) Frisch, M. J.; Trucks, G. W.; Schlegel, H. B.; Scuseria, G. E.; Robb, M. A.; Cheeseman, J. R.; Zakrzewski, V. G.; Montgomery, J. A. .; Stratmann, R. E.; Burant, J. C.; Dapprich, S.; Millam, J. M.; Daniels, A. D.; Kudin, K. N.; Strain, M. C.; Farkas, O.; Tomasi, J.; Barone, V.; Cossi, M.; Cammi, R.; Mennucci, B.; Pomelli, C.; Adamo, C.; Clifford, S.; Ochterski, J.; Petersson, G. A.; Ayala, P. Y.; Cui, Q.; Morokuma, K.; Malick, D. K.; Rabuck, A. D.; Raghavachari, K.; Foresman, J. B.; Cioslowski, J.; Ortiz, J. V.; Stefanov, B. B.; Liu, G.; Liashenko, A.; Piskorz, P.; Komaromi, I.; Gomperts, R.; Martin, R. L.; Fox, D. J.; Keith, T.; Al-Laham, M. A.; Peng, C. Y.; Nanayakkara, A.; Gonzalez, C.; Challacombe, M.; Gill, P. M. W.; Johnson, B.; Chen, W.; Wong, M. W.; Andres, J. L.; Gonzalez, C.; Head-Gordon, M.; Replogle, E. S.; Pople, J. A. *Gaussian 98*; Gaussian, Inc.: Pittsburgh, PA, 1998.
(17) (a) Lee, C.; Yang, W.; Parr, R. G. *Phys. Rev. B* **1988**, *37*, 785. (b) Becke, D. *J. Chem. Phys.* **1993**, *98*, 5648.
(18) Ehlers, A. W.; Böhme, M.; Dapprich, S.; Gobbi, A.; Höllwarth, A.; Jonas, V.; Köhler, K. F.; Stegmann, R.; Veldkamp, A.; Frenking, G. *Chem. Phys. Lett.* **1993**, *208*, 111.
(19) Hay, P. J.; Wadt, W. R. *J. Chem. Phys.* **1985**, *82*, 299.
(20) Huzinaga, S. *Physical Sciences Data 16, Gaussian Basis Sets for Molecular Calculations*; Elsevier: Amsterdam, 1984.
(21) Wadt, W. R.; Hay, P. J. *J. Chem. Phys.* **1985**, *82*, 284.
(22) Fukui, K.; Kato, S.; Fujimoto, H. *J. Am. Chem. Soc.* **1975**, *97*, 1.
(23) Saillard, J.-Y.; Hoffmann, R. *J. Am. Chem. Soc.* **1984**, *106*, 2006.
(24) Pauling's values are presented. For example, see: *The Elements*, 2nd ed.; Emsley, J., Ed.; Oxford University Press: New York, 1991.
(25) Fischer, E. O.; Maasbol, A. *Angew. Chem., Int. Ed. Engl.* **1964**, *3*, 580.

Scheme 1

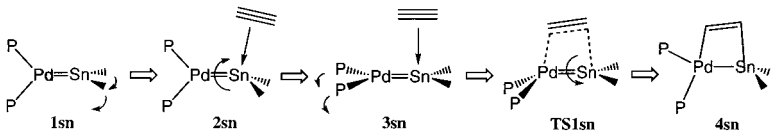

strength of the π-back-donation. The stannylene complex **1sn** would be most likely a Fisher type because the π-back-donation is weak and the electrons are thought to be relatively localized on the dπ orbital of the Pd rather than on the pπ orbital of the Sn. When the Sn atom is replaced by the C atom, the character of the complex **1** would be changed from Fisher to Schrock with a increase in the π-back-donation in the order C > Si > Sn. The order of the strength of the π-back-donation is also supported by the fact that the energy level of the unoccupied p orbital of the XH_2 fragment is lowered in the order C > Si > Sn and shifts closer to the energy level of the occupied dπ orbital of the Pd of the $(PH_3)_2Pd$ fragment. Therefore, the character of the occupied dπ orbital of Pd is more largely reflected in the order Sn > Si > C in the formed molecular orbital with the unoccupied p orbital of X in the $(PH_3)_2Pd{=}XH_2$ complex, which suggests that the electron is more localized on the dπ orbital of Pd with the same order.

3.2. C≡C Bond Activation. The reaction of $(PH_3)_2Pd{=}SnH_2$ **1sn** with C_2H_2 to produce the 1,2-palladastannete complex **4sn** has been thought to be the favorable path in the first process of the catalytic cycle of the stannole formation,[13] as mentioned in the Introduction. Although we have already reported in the previous paper the structures of the intermediates and the transition state included in this elementary reaction step and their energies,[13] those structures and the potential energy surface of the reaction were recalculated with the higher quality basis set including a polarization function for the P atom of the spectator PH_3 ligands and the H atom of ethyne and stannylene, and then similar results were obtained as presented in Figure 3.

The incoming ethyne first weakly coordinates not to the Pd atom but to the Sn atom to form **2sn** by only electron donation from the pπ orbital of the ethyne to the unoccupied p orbital of the Sn with the slight bend of the two hydrogens attached to the Sn atom. The pπ orbital of Sn inclines away from the dπ orbital of Pd due to the steric repulsion between the ethyne and the PH_3 ligand to weaken the π-back-donation from the Pd dπ orbital to the Sn pπ orbital and make the rotation of the $(PH_3)_2Pd$ group around the Pd−Sn axis facile. In fact, the energy required for the rotation around the M−Sn bond to form **3sn** was only 2.2 kcal/mol, even with the polarization function for the P atoms.[27] The rotation of the $(PH_3)_2Pd$ group by 90° around the M−Sn bond further weakens the π-back-donation from the dπ orbital of Pd to the p orbital of Sn, as shown by the M−Sn bond distance in **3sn** being longer by 0.052 Å than that in **2sn**. Thereby, the electron donation from the ethyne π orbital to the unoccupied Sn p orbital becomes stronger, so that the Sn−C distances become

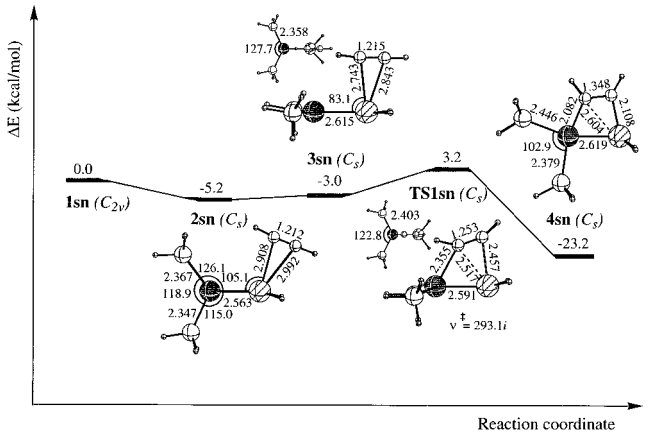

Figure 3. B3LYP/I potential energy surface (in kcal/mol) of the activation of the ethyne C≡C π bond at the Pd═Sn bond of the $(PH_3)_2Pd{=}SnH_2$ complex **1sn** with the optimized structures (in Å and deg) of the intermediates **2sn** and **3sn**, the transition state **TS1sn**, and the product **4sn** at the B3LYP/I level. The top views are also displayed for **3sn** and **TS1sn**. The value of the imaginary frequency (cm^{-1}) is presented for the transition state **TS1sn**.

shorter and the ethyne inclines back to come closer to the Pd atom. Here, the C≡C π bond of ethyne is initially activated by the electron donation. The electron back-

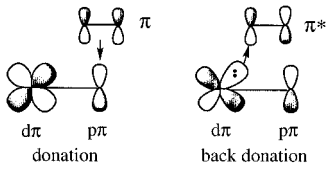

donation from the Pd dπ orbital to the ethyne π^* orbital finally breaks the ethyne C≡C π bond to form the M−C bond through the transition state **TS1sn**, where the ethyne bridges over the Pd−Sn bond. The slight bend of the electron donative phosphine ligands in **TS1sn** enhances the back-donation. After passing through **TS1sn**, the $(PH_3)_2Pd$ group rotates back to produce **4sn**. The single bond Pd−Sn in **4sn** is longer by 0.097 Å than the double bond Pd−Sn in **1sn**. The reaction is 23.2 kcal/mol exothermic, as shown in Figure 3. The potential energy surface starting from **1sn** to from **4sn** is quite smooth, requiring a small energy barrier of only 6.2 kcal/mol for the C≡C π bond activation from **3sn** to **4sn**, which is successfully achieved by the stepwise reaction, with the efficient movement of the phosphine ligands (Scheme 1) playing a key role in the orbital interactions mentioned above. Without the rotation of the $(PH_3)_2Pd$ group around the Pd−Sn axis in **2sn**, no transition state was located.

When the chelate ligand $H_2PC_2H_4PH_2$ is used instead of the PH_3 ligands, the potential energy surface is stabilized by more than 10 kcal/mol due to the small bite angle ∠P−Pd−P of about 84−88° throughout the reaction, and its features are slightly changed due to

(26) Schrock, R. R. *J. Am. Chem. Soc.* **1974**, *96*, 6796.
(27) No essential energy barrier for the rotation of the $(PH_3)_2Pd$ group around the M−Sn bond was found by following the reaction coordinate.

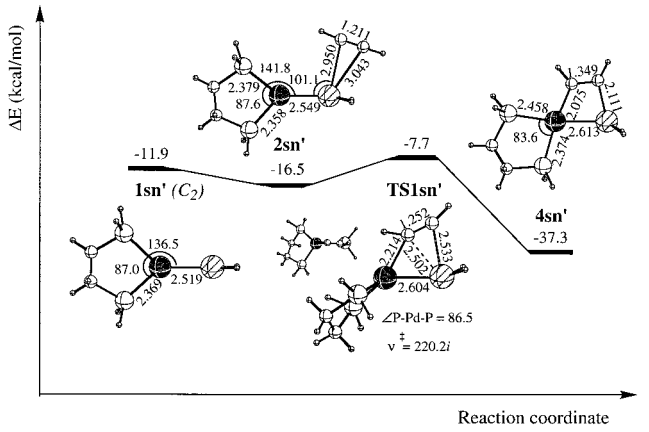

Figure 4. B3LYP/I potential energy surface (in kcal/mol) of the activation of the ethyne C≡C π bond at the Pd═Sn bond of the $(H_2PC_2H_4PH_2)$Pd═SnH_2 complex **1sn′** with the optimized structures (in Å and deg) of the intermediate **2sn′**, the transition state **TS1sn′**, and the product **4sn′** at the B3LYP/I level. The top view is also displayed for **TS1sn′**. The value of the imaginary frequency (cm^{-1}) is presented for the transition state **TS1sn′**.

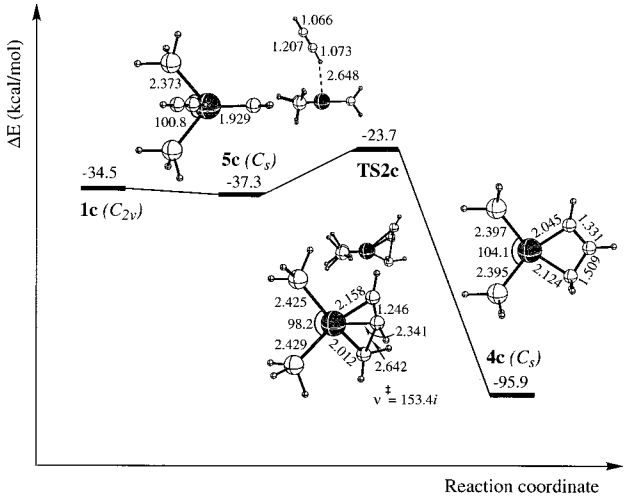

Figure 5. B3LYP/I potential energy surface (in kcal/mol) of the activation of the ethyne C≡C π bond at the Pd═C bond of the $(PH_3)_2$Pd═CH_2 complex **1c** with the optimized structures (in Å and deg) of the intermediate **5c**, the transition state **TS2c**, and the product **4c** at the B3LYP/I level. The side views are also displayed for **5c** and **TS2c**. The value of the imaginary frequency (cm^{-1}) is presented for the transition state **TS2c**.

the lack of the inetermediate **3sn′**. The potential energy surface together with the optimized structures of the reactant **1sn′**, intermediate **2sn′**, transition state **TS1sn′**, and product **4sn′** is presented in Figure 4.

The Pd═Sn bond distance in the stannylene complex **1sn′** is somewhat shorter compared with that in **1sn** due to the stronger π-back-donation from the occupied dπ orbital of Pd to the unoccupied pπ orbital of Sn, the dπ orbital of Pd being more enhanced by the small ∠P−Pd−P angle of 87.0°. The structure **1sn′** is 11.9 kcal/mol more stable in energy than **1sn**. The stronger π-back-donation is also reflected in the structure and the stability of **2sn′**; the Sn−C distances are 0.04−0.05 Å longer and the stabilization, which is obtained by the interaction with ethyne by the donation from the ethyne pπ orbital to the unoccupied p orbital of Sn, is 0.6 kcal/mol smaller compared with those of **2sn**. It should be noted that the intermediate **3sn** found in the $(PH_3)_2$-Pd═SnH_2 system does not exist as an equilibrium structure due to the strong π-back-donation from the Pd dπ orbital to the Sn pπ orbital. Therefore, the energy barrier from **2sn′** to **TS1sn′** is 8.8 kcal/mol and is larger by 2.2. kcal/mol than that from **3sn** to **TS1sn** in the $(PH_3)_2$Pd═SnH_2 system. In **TS1sn′**, the $(H_2PC_2H_4PH_2)$-Pd group similarly rotates around the Pd−Sn axis by about 90° and the back-donation from the Pd dπ orbital to the ethyne pπ* orbital breaks the C≡C π bond. The subsequent rotation of the $(H_2PC_2H_4PH_2)$Pd group produces the product **4sn′**.

The activation activity remarkably increases when the Sn atom is replaced by the Si atom. The reaction becomes downhill and proceeds without energy barrier because of the large exothermicity (43.5 kcal/mol). However, the same consecutive stepwise reaction, i.e., (i) the η^2-ethyne coordination to the Si atom, (ii) the rotation of the $(PH_3)_2$Pd group around the Pd−Si axis with the incipient Pd−C and Si−C bond formation, and (iii) the rotation back of the $(PH_3)_2$Pd group with the complete formation of the Pd−C and Si−C bonds, was observed by following the reaction coordinate.

If X is C, the mechanism is completely different. The incoming ethyne is first bound not to the C atom but to the Pd atom as presented in Figure 5 . Since the electron localized on the p orbital of the C atom (see section 3.1) prevents ethyne from coordinating to the C atom by the electron donation from the pπ orbital of ethyne to the p orbital of the C atom, ethyne is very weakly bound to the Pd atom by the electron donation from the C−H σ orbital of ethyne to the hybridized dσ+sp orbital of Pd, as shown by the C−H bond distance being stretched by only 0.007 Å. Another equilibrium structure with almost the same stability where ethyne is bound to the bridge site of the Pd═C in the P−Pd−P plane by a similar structural configuration was also found, but it was not on the reaction coordinate connected to the product **4c**. The ethyne slides into the P−Pd−C(carbene) plane with the rotation of the CH_2 moiety to produce two kinds of orbital interactions for the C≡C π bond breaking in the transition state **TS2c**, as illustrated below: (i) the electron donation from the ethyne π orbital to the Pd dπ orbital and (ii) the back-donation from the C pπ orbital to the ethyne π* orbital. Here, the dπ orbital of

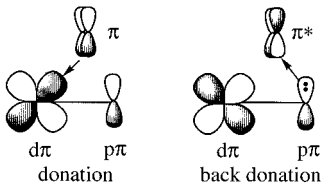

Pd perpendicular to the P−Pd−P plane is available. The deformed structure of the transition state **TS2c** is arranged to form the planar structure of the product **4c** with C_s symmetry. This reaction obviously differs from the stepwise reaction seen for X = Sn, Si. Despite the large exothermicity of the reaction (61.4 kcal/mol), the energy barrier of 13.6 kcal/mol was about 2 times larger than that for X = Sn, which originates from the different reaction mechanism.

3.3. O−H Bond Activation. Also, in the activation of the water O−H bond at the Pd═Sn bond of the $(PH_3)_2$-

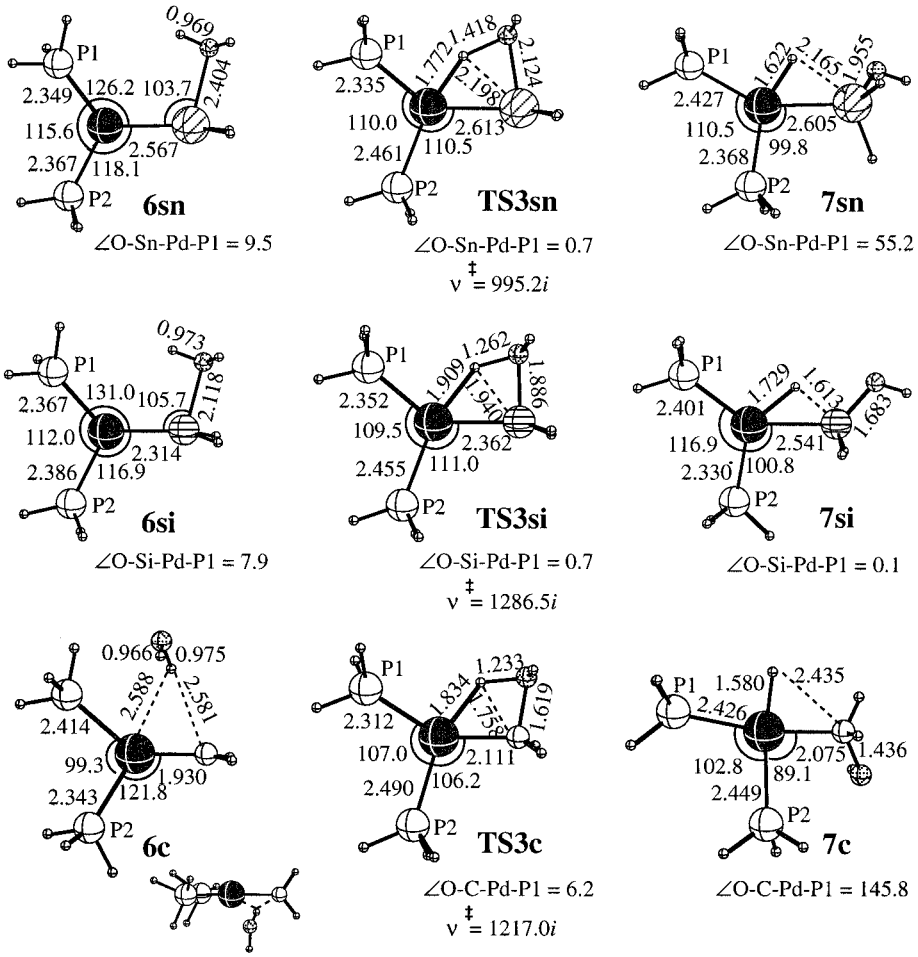

Figure 6. B3LYP/I-optimized structures (in Å and deg) of the intermediates **6**, transition states **TS3**, and the products **7** for the activation of the water O−H bond at the Pd═X bonds (X = Sn, Si, C) of the $(PH_3)_2Pd{=}XH_2$ complexes **1**. The top view is also displayed for **6c**. The values of the imaginary frequencies (cm^{-1}) are presented for the transition states **TS3**.

Pd═SnH_2 complex to lead to the product **7sn**, the strong electron donor oxygen of water first coordinates to the Sn with an O−Sn distance of 2.404 Å by the electron donation of the lone pair electron of the oxygen to the unoccupied p orbital of Sn to produce the intermediate **6sn**, as presented in Figure 6.

To reduce the π-back-donation from the occupied dπ orbital of Pd to the unoccupied pπ orbital of Sn and the repulsion between the lone pair electron of the H_2O oxygen and the electron localized on the dπ orbital of Pd, the p orbital of Sn inclines with the angle ∠O−Sn−Pd of 103.7° and the H_2O-coordinated SnH_2 rotates by 9.5° around the Pd−Sn axis in **6sn**. As a result, the Pd−Sn bond in **6sn** is stretched by 0.045 Å compared with that in **1sn**. The positive charge of the hydrogen of the coordinated H_2O (0.351 e) in **6sn** increases by 0.045 e compared with that of the free H_2O (0.306 e). The interaction of the H_2O oxygen with Sn by the electron donation induces an electron flow from the H_2O hydrogen to the electron-deficient p orbital of Sn through the H−O−Sn linkage. On the other hand, the nucleophilicity of the Pd is enhanced because the electrons contributing to the back-donation to the Sn p orbital is more localized on the Pd dπ orbital by this electron flow. In the transition state **TS3sn**, the $(PH_3)_2Pd$ group does not rotate around the Pd−Sn axis as shown by the quite small ∠O−Sn−Pd−P1 dihedral angle of 0.7° for two reasons: (i) the H_2O oxygen can strongly coordinate to the Sn atom without rotation, and (ii) the nucleophilicity of Pd is reduced by the rotation. Instead, two PH_3 ligands slightly rotate counterclockwise around the Pd atom on the P−Pd−P plane, keeping the ∠P−Pd−P angle of about 110°. The O−Sn bond in **TS3sn**, which is only 8.6% longer than that in the product **7sn**, is nearly formed and the Pd−Sn distance of 2.613 Å is already long, indicating a single bond. Thus, after the coordination of the H_2O oxygen to the Sn atom, an electrophilic attack of the positively charged H_2O hydrogen to the Pd initiates the reaction, and the H_2O hydrogen migrates as a proton to the Pd atom and the OH^- coordinates to the Sn atom, as presented below, where the valence of Pd changes from Pd(0) to Pd(II) to make a hydride. The O−H bond distance of 1.418 Å in

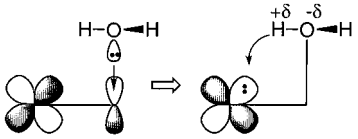

TS3sn is long, indicating heterolytic cleavage, while the Pd−H bond distance of 1.772 Å is short. After passing through the transition state **TS3sn**, the $Sn(OH)(H)_2$ group rotates around the Pd−Sn axis to produce the product **7sn**. Similar rotation has been experimentally observed by X-ray analysis for the product.[14] In the

product **7sn**, the Pd−H bond inclines toward the Sn atom with a relatively short H−Sn distance of 2.165 Å, indicating a bridge of the hydrido ligand over the Pd−Sn bond. Since the electron for the Pd−H bond is delocalized in the Pd−H−Sn region by the bridge of the hydrido ligand, the electron donation of the PH_3 trans to the hydrido to the Pd is promoted, giving a Pd−P2 bond distance that is shorter by 0.059 Å than the Pd−P1 bond distance. The mechanism experimentally proposed by Pörschke et al.[14] on the basis of only the experimental fact that an intermediate with H_2O coordinated to Sn was not detected is as follows: the $[(PH_3)_2Pd(H)SnH_2]^+$ cation complex and OH^- anion are formed first by the protonation at the nucleophile Pd, and then OH^- coordinates to the electrophile Sn. However, the ability of the solvation of SnH_2 is not completely lost by the coordination of SnH_2 to the Pd atom but rather still strong, although it would be somewhat reduced. In fact, the stable intermediate **6sn** with H_2O coordinated to Sn exists as an equilibrium structure. Therefore, the reaction path via the H_2O-coordinated intermediate **6sn**, **1sn→6sn→TS3sn→7sn**, would be quite plausible.

The same proton transfer reaction is also considered for X = Si. One can readily notice at a glance that the structural features of the H_2O-coordinated intermediates **6**, the transition states **TS3**, and the products **7** for X = Sn, Si are similar to each other aside from the differences in the values of the geometrical parameters. In **6si**, the angle ∠O−Si−Pd of 105.7° is slightly larger than that in **6sn**, while the dihedral angle ∠O−Si−Pd−P1 of 7.9° is slightly smaller than that in **6sn**. The positive charge of the hydrogen of the coordinated H_2O was slightly larger for X = Si than for X = Sn. The transition state **TS3si** is shifted to the reactant side compared with **TS3sn**, as shown by the obviously longer Pd−H distance of 1.909 Å and the shorter O−H distance of 1.262 Å. It should be noted that in the product **7si** the Pd−H distance of 1.729 Å is longer than the Si−H distance of 1.613 Å, which suggests that the delocalized electron in the Pd−H−Si bridge is relatively more localized in the H−Si part rather than in the Pd−H part. An electrostatic interaction of the protonic hydrido with the lone pair electron of oxygen gives a structure having almost C_s symmetry. The Pd−P2 bond distance of 2.330 Å is obviously shorter than the Pd−P1 bond distance of 2.401 Å for the same reason as the case of X = Sn mentioned above. Compared with the corresponding angles in **7sn**, in **7si**, the angle ∠P−Pd−P is larger for sterical reasons since the angle ∠H−Pd−Si is smaller.

In the case of X = C, the H_2O oxygen cannot coordinate to the C atom by the donation of the lone pair electron to the p orbital of the C atom in **6c** because the electron contributing to the interaction between the Pd and C atoms by the back-donation from the dπ orbital of Pd to the pπ orbital of C is localized on the pπ orbital of C (see section 3.1). The H_2O hydrogen, which has positive charge, bridges over the electron-rich Pd=C by a weak electrostatic interaction. The Pd−C distance in **6c** is only slightly stretched compared with that in **1c**. In the transition state **TS3c**, the O−H bond breaking takes place homolytically, which is different from the proton-transfer reaction for X = Sn, Si, by the electron donation from the O−H σ orbital to the dπ orbital of Pd and back-donation from the p orbital of C to the O−H σ^* orbital:

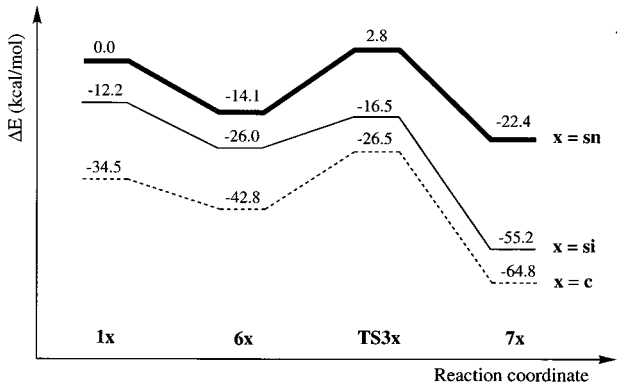

Figure 7. B3LYP/I potential energy surfaces (in kcal/mol) of the activation of the water O−H bond at the Pd=X bonds (X = Sn, Si, C) of the $(PH_3)_2Pd{=}XH_2$ complexes **1**. The boldface, normal, and dotted lines are for X = Sn, Si, C, respectively.

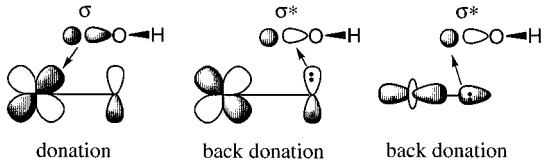

As shown by the short H−C distance of 1.758 Å and the Pd−C bond being longer by 0.036 Å than the single Pd−C bond in the product **7c**, another back-donation from the Pd−C σ orbital to the O−H σ^* orbital also contributes to stabilize the transition state. The product **7c** has a square-planar structure without the interaction of the hydrido H with the C atom. The OH substituent on C is away from the hydrido ligand with the large ∠O−C−Pd−P1 dihedral angle of 145.8° to avoid the repulsive contact of its lone pair electron on oxygen with the anionic hydrido hydrogen. The strong bonding of the hydrido hydrogen with the Pd atom, which is shown by the short Pd−H distance of 1.580 Å, weakens the donation of PH_3 trans to the hydrido. Consequently, the Pd−P2 distance of 2.449 Å is longer than the Pd−P1 distance of 2.426 Å, which is different from the case for X = Sn, Si.

The potential energy surfaces of the reactions $(PH_3)_2Pd{=}XH_2$ (X = Sn, Si, C) **1** + H_2O are presented together in Figure 7. For X = Sn, the H_2O-coordinated intermediate **6sn** is 14.1 kcal/mol more stable in energy than the stannylene complex **1sn**. After the formation of **6sn**, the reaction proceeds passing through the transition state **TS3sn** with an energy barrier of 16.9 kcal/mol to produce the product **7sn**. The potential energy surface for X = Si is shifted down compared with that for X = Sn. It should be noted here that the transition state **TS3si** is lower in energy than the reactant **1si,** in contrast to the case of X = Sn. The energy barrier is reduced to 9.5 kcal/mol due to the larger exothermicity, suggesting a higher activation activity. The potential energy surface for X = C is further shifted down. The energy barrier of 16.3 kcal/mol is as large as that for X = Sn despite the large exothermicity of 30.3 kcal/mol, because the transition state **TS3c** is less stable by 8.0 kcal/mol than the reactant **1c**, which would originate from the different reaction mechanism.

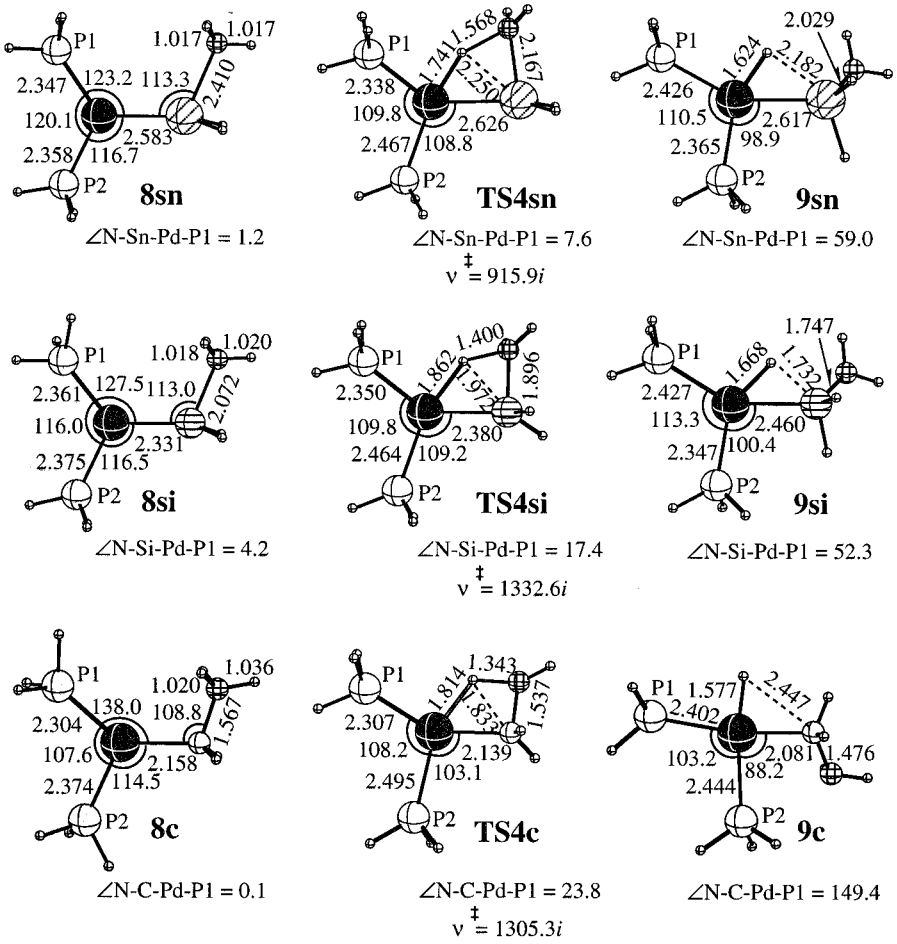

Figure 8. B3LYP/I-optimized structures (in Å and deg) of the intermediates **8**, transition states **TS4**, and the products **9** for the activation of the ammonia N−H bond at the Pd=X bonds (X = Sn, Si, C) of the $(PH_3)_2Pd{=}XH_2$ complexes **1**. The values of the imaginary frequencies (cm^{-1}) are presented for the transition states **TS4**.

Even if the PH_3 ligands are replaced by the chelate ligand $H_2PC_2H_4PH_2$ or methanol is used instead of water in the reaction system with X = Sn, no significant changes were found in both geometrical features of the equilibrium structures and the transition states and the shape of the potential energy surfaces (see Figure S-1 and S-2 presented as a Supporting Information).[28]

3.4. N−H Bond Activation. The NH_3-coordinated intermediates **8**, similar to the H_2O-coordinated intermediates **6sn** and **6si** in the activation of the water O−H bond, was also found in the activation of the ammonia N−H bond independent of the atom X as presented in Figure 8. The donation of the lone pair electron of NH_3, being larger than that of H_2O, which would be ascribed to the sequence of the electronegativity O(3.44) > N(3.04),[24] is reflected in some geometrical parameters and also gives **8c**. The N−Sn and N−Si axes in **8sn** and **8si**, respectively, incline due to the slight sp^3 hybridization on the Sn and Si atoms in addition to the electrostatic repulsion between the electron in the N−Sn or N−Si bond and the localized electron on the Pd dπ orbital. The bond angles ∠N−Sn−Pd in **8sn** and ∠N−Si−Pd in **8si** are larger by 7−10° than the corresponding angles in **6sn** and **6si**, respectively. The distances, Pd−Sn in **8sn** and Pd−Si in **8si**, are longer by 0.016−0.017 Å than those in **6sn** and **6si**, and the ∠P−Pd−P angles in **8sn** and **8si** are also larger by 4−5° than those in **6sn** and **6si**, respectively, since the π-back-donation from the dπ orbital of the Pd atom to the pπ orbital of the X atom is more weakened by the donation of the lone pair electron of NH_3 to the p orbital of the X atom, being larger than that of H_2O. In **8c**, the N−C bond is almost formed as shown by the short N−C distance of 1.567 Å, which is only 6.1% stretched compared with that in the product **9c**. The Pd−C bond distance of 2.158 Å is already long, indicating a single bond, and the sp^3 hybridization on C having tetrahedral structure is almost completed. The positive charge of the hydrogen of the coordinated NH_3 in **8** remarkably increased compared with that of the hydrogen of the free NH_3 with the order C > Si > Sn.

The similar proton-transfer mechanism proposed for the case of H_2O with X = Sn, Si is also considered for the case of NH_3 independent of the atom X; the coordination of NH_3 to the X atom by the strong donation of the lone pair electron of nitrogen to the p orbital of the X atom in **8** enhances the positive charge of the NH_3 hydrogen and simultaneously the nucleophilicity of the Pd atom, and then subsequently, the hydrogen migrates as a proton to the Pd atom as illustrated below, passing through the transition state **TS4**. The formation of the N−X bonds is almost com-

(28) The angles ∠O−Sn−Pd in **6sn** and ∠O−Sn−Pd−P1 in **7sn** somewhat decreased when the chelate ligand $H_2PC_2H_4PH_2$ was used instead of the PH_3 ligands because the small bite angle of the $H_2PC_2H_4PH_2$ ligand relaxes the sterical stress among the ligands.

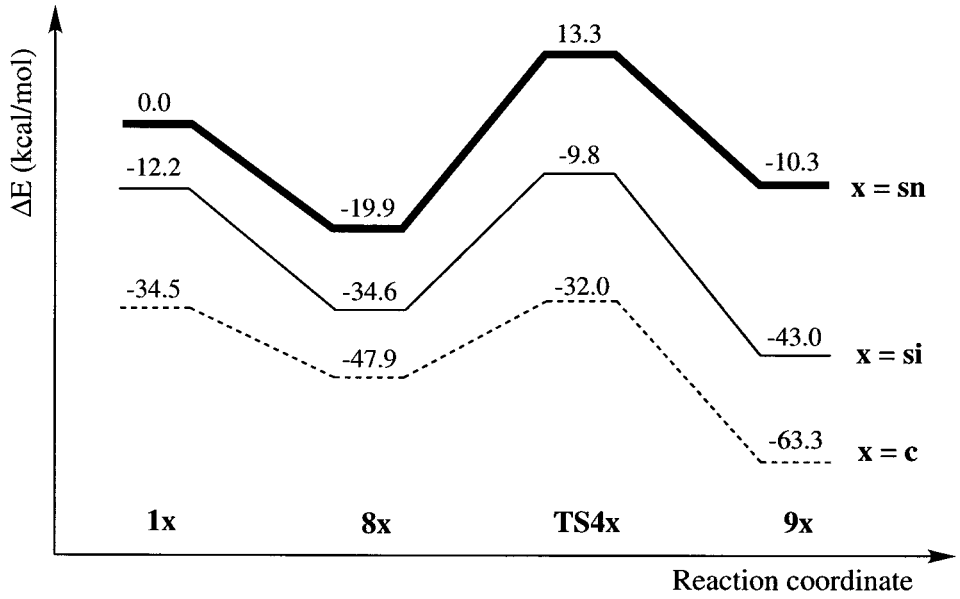

Figure 9. B3LYP/I potential energy surfaces (in kcal/mol) of the activation of the ammonia N−H bond at the Pd═X bonds (X = Sn, Si, C) of the $(PH_3)_2Pd{=}XH_2$ complexes **1**. The boldface, normal, and dotted lines are for X = Sn, Si, C, respectively.

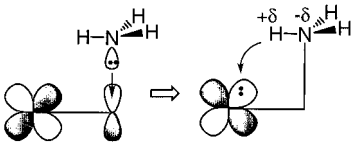

pleted at least in the transition state **TS4**, as shown by the short N−X distances in **TS4**, which are only 4−8% stretched compared with those in the product **9**. The Pd−X bonds in **TS4** are already long, indicating a single bond. It should also be noted that the N−H distances are relatively long while the Pd−H distances are short in **TS4**. The structures of **TS4** largely deviate from the C_s symmetry because the rotation of the XH_2 group with the activated NH_3 around the Pd−X axis already starts in the transition state, which is different from the case of H_2O. This would be ascribed to the easiness of the rotation of the $X(NH_3)H_2$ group around the Pd−X axis. One will also find the trend that the transition state **TS4** is more shifted to the reactant side with the order C > Si > Sn.

As well as **7sn** and **7si** the products **9sn** and **9si** give a H-bridge structure at the Pd−X bond, its character being reduced with the decrease in the electrophilicity of the X atom by the attached NH_2, being more electron donative than OH. On the other hand, in **9c**, the hydrido ligand does not bridge over the Pd−C bond and the Pd−H bond distance of 1.577 Å is shorter than those in **9sn** and **9si**, which is similar to the case of H_2O. The dihedral angle ∠N−C−Pd−P1 of 149.4° is also the largest in **9c**. In **9sn** and **9si**, the Pd−P2 bond distances are shorter than the Pd−P1 bond distances, while in **9c** the Pd−P2 bond distance is longer than the Pd−P1 bond distance due to the aforementioned trans influence of the hydrido ligand (see section 3.3).

The potential energy surfaces of the reactions $(PH_3)_2Pd{=}XH_2 + NH_3$ (X = Sn, Si, C), **1**→**8**→**TS4**→**9**, are presented in Figure 9. The stability of the NH_3-coordinated intermediates **8** for X = Sn, Si, C is larger than that of the corresponding H_2O-coordinated intermediates **6**,[29] because the donation of the lone pair electron of NH_3 is stronger than that of H_2O. On the other hand, the stability of the products **9** is smaller than that of the corresponding products **7**. Therefore, the reaction is less exothermic and the energy barrier is larger compared with the case of H_2O. That no activation activity of the Pd═Sn bond for NH_3 was found experimentally, in sharp contrast to the high activation activity for H_2O,[14] would be reasonably understood by the energy barrier being two times larger for NH_3 than for H_2O in the reaction system with X = Sn. The potential energy surface is stabilized in the order C > Si > Sn, which is similar to the case of H_2O, and the energy barrier decreases with the same order. The energy barrier of 33.2 kcal/mol required in the case of X = Sn was reduced to 24.8 kcal/mol in the case of X = Si since the exothermicity of the reaction increases to 30.8 kcal/mol. The energy barrier further reduced to 15.9 kcal/mol in the case of X = C due to the small stabilization of **8c**, although the stability of the transition state **TS4c** and the product **9c** relative to the reactant **1c** is almost the same as that in the case of X = Si. This reduction of the energy barrier suggests an reaction activity for the N−H bond activation in the system with X = C.

4. Concluding Remarks

The activation of chemical bonds at the double bond between the metal and ligand is unique, and the role of the ligand in the reaction is quite interesting. In this study, the mechanism of the activation of the C≡C π bond of ethyne, the O−H bond of water, and the N−H bond of ammonia at the Pd═X (X = Sn, Si, C) bonds of the model $(PH_3)_2Pd{=}XH_2$ complexes **1** to produce the products $(PH_3)_2Pd(CH{=}CH)XH_2$ (*Pd−X*) **4**, $(PH_3)_2Pd(H)X(OH)H_2$ **7**, and $(PH_3)_2Pd(H)X(NH_2)H_2$ **9**, respectively, was theoretically examined using the density

(29) This calculation result supports the experimental fact that the NH_3 adduct was successfully observed,[15] but the H_2O adduct was not.[14]

functional method (B3LYP), and it was found that the reaction mechanism significantly depends on both substrate and atom X of the complex **1** as follows.

The activation of the C≡C π bond of ethyne at the Pd═Sn bond, which is initiated by a weak η^2-interaction of the C≡C π bond with the Sn atom of the ligand, is accompanied by the rotation of the $(PH_3)_2Pd$ group around the Pd−Sn axis to make the reaction facile. Therefore, the potential energy surface is quite smooth with a small energy barrier of only 6.2 kcal/mol. When X is Si, the reaction, which also takes the same mechanism, becomes downhill due to the large exothermicity. On the other hand, in the case of X = C, the reaction proceeds by a different mechanism without the coordination of the C≡C π bond to the C atom with the large energy barrier of 16.3 kcal/mol.

In the activation of the O−H bond of H_2O at the Pd═Sn bond, the coordination of the H_2O oxygen to the Sn atom initiates the reaction, and subsequently, the hydrogen is transferred to the Pd atom as a proton by heterolytic cleavage. Also, at the Pd═Si bond the same heterolytic cleavage of the O−H bond takes place, the energy barrier being reduced to about half of that for X = Sn. However, at the Pd═C bond, a homolytic cleavage of O−H bond occurs, requiring almost the same energy barrier for X = Sn.

On the other hand, the activation of the N−H bond of NH_3 takes the proton-transfer mechanism with the coordination of the NH_3 nitrogen to the X atom independent of the atom X. In agreement with the experimental finding that no activation of the N−H bond of NH_3 takes place at the Pd═Sn bond while the activation of the O−H bond of H_2O readily occurs under the same reaction conditions, the energy barrier of 33.2 kcal/mol for NH_3 in the system with X = Sn was about 2 times larger than the corresponding energy barrier of 16.9 kcal/mol for H_2O. However, when X is C the energy barrier was reduced to 15.9 kcal/mol, suggesting an activation activity for NH_3, the sequence of the energy barrier being Sn > Si > C.

Acknowledgment. The calculations were in part carried out at the Computer Center of the Institute for Molecular Science, Japan. T.M. was partly supported by the Grants-in Aid from the Ministry of Education, Science, Sports, and Culture, Japan.

Supporting Information Available: Listings giving the optimized Cartesian coordinates of all equilibrium structures and transition states presented in this paper and the potential energy surfaces of the reactions $(H_2PC_2H_4PH_2)Pd═SnH_2 + H_2O$ (Figure S-1) and $(PH_3)_2Pd═SnH_2 + CH_3OH$ (Figure S-2), together with the optimized structures. This material is available free of charge via the Internet at http://pubs.acs.org.

OM001000A